

Catalysis Science & Technology

Accepted Manuscript



This is an *Accepted Manuscript*, which has been through the Royal Society of Chemistry peer review process and has been accepted for publication.

Accepted Manuscripts are published online shortly after acceptance, before technical editing, formatting and proof reading. Using this free service, authors can make their results available to the community, in citable form, before we publish the edited article. We will replace this *Accepted Manuscript* with the edited and formatted *Advance Article* as soon as it is available.

You can find more information about *Accepted Manuscripts* in the [Information for Authors](#).

Please note that technical editing may introduce minor changes to the text and/or graphics, which may alter content. The journal's standard [Terms & Conditions](#) and the [Ethical guidelines](#) still apply. In no event shall the Royal Society of Chemistry be held responsible for any errors or omissions in this *Accepted Manuscript* or any consequences arising from the use of any information it contains.

Deactivation Mechanism of SO₂ on the Cu/SAPO-34

NH₃-SCR Catalysts: Structure and Active Cu²⁺

Meiqing Shen^{a, b, c}, Huaiyou Wen^a, Teng Hao^a, Tie Yu^a, Dequan Fan^a, Jun Wang^a,
Wei Li^{d*}, Jianqiang Wang^{a*}

^a Key Laboratory for Green Chemical Technology of State Education Ministry,
School of Chemical Engineering & Technology, Tianjin University, Tianjin
300072, PR China

^b State Key Laboratory of Engines, Tianjin University, Tianjin 300072, PR China

^c Collaborative Innovation Center of Chemical Science and Engineering, Tianjin
300072, China

^d General Motors Global Research and Development, Chemical Sciences and
Materials Systems Lab, 3500 Mound Road, Warren, MI 48090, USA

* Corresponding author: Jianqiang Wang

Postal address:

School of Chemical Engineering and Technology, Tianjin University, 92 Weijin Road,
Nankai District, Tianjin 300072, China

Email: wangjianqiang@tju.edu.cn; wei.1.li@gm.com

Tel./ Fax.: (+86) 22-27892301

Abstract:

The deactivation mechanism of Cu/SAPO-34 ammonia selective catalytic reduction catalysts (NH₃-SCR) by SO₂ poisoning has been systematically investigated using a range of analytical techniques in order to study the influence on both the zeolitic framework and the active Cu²⁺ ions. The different sulfate samples were obtained by SO₂ poisoning over Cu/SAPO-34 NH₃-SCR catalysts as functions of the time and concentration in the feed. The obtained results reveal that the SO₂ poisoning could seriously decrease the NO conversion during the whole temperature range (100 °C-500 °C). The XRF result shows that there is almost no sulfur existing on the

SAPO-34 support. The *ex-situ* DRIFTS and BET results expose that the SO₂ poisoning does a less pronounced affect on its framework structure. The TPR and EPR results demonstrate that SO₂ poisoning does a significant influence on the coordination environment and the content of the active isolated Cu²⁺ species. The kinetic results demonstrate the SO₂ poisoning does not influence the apparent activation energy (E_a) of NH₃-SCR reaction over Cu/SAPO-34 catalysts. The decline of the NH₃-SCR activity is due to the reduction of the number of isolated Cu²⁺ ions.

Key words: Cu/SAPO-34; SO₂ poisoning; Active Cu²⁺; Deactivation Mechanism

1. Introduction

World-wide news on poor air quality in Chinese cities was quite common since 2013. Some of the leading contributors are the pollutants emitted from increasing automobiles. These environmental problems have resulted in a continuous decrease of the allowed NO_x concentrations due to stringent emission regulations. Ammonia selective catalytic reduction (NH₃-SCR) was considered as the technology with the highest potential to meet strict future diesel emissions standards in mobile applications.

Well established NH₃-SCR technique uses either V₂O₅/WO₃-TiO₂ or Zeolite based catalysts. Zeolite-based catalysts promoted by transition metal such as Fe and Cu represent an excellent solution to overcome the stability problems of V₂O₅-based catalysts but may show disadvantages in stability after hydrothermal ageing and sulphur poisoning^[1-3]. Recently, Bull and Kwak et al^[4-7] reported the small-pore zeolite (~3.8 Å) with the CHA structure show significant promise as the new leading candidate among zeolite formulations compared to the Cu/ZSM-5 and Cu/Beta. Bull and Andersen et al^[8,9] firstly reported the NH₃-SCR activity of Cu/SAPO-34 catalyst. In addition, Fickel and others found that Cu/SAPO-34 catalysts perform superior NH₃-SCR activity and prominent hydrothermal stability at 750 °C to that of Cu/zeolites was related to their unique microporous structure^[5,7]. Meanwhile,

previous researches ^[6,10-12] proved the isolated Cu^{2+} species are the SCR active sites by EXAFS and kinetic tests.

A major problem in practical applications of SCR catalysts has been their deactivation by different components in the exhaust gas, which accumulate on the catalyst surface ^[13,14]. Deactivation can also result from competitive adsorption of certain molecules on SCR sites, thereby inhibiting the SCR reaction. The main focus hereby was on the effect of sulfur poisoning. Because of its high chemical binding strength and the oxidative conditions in the exhaust stream, sulfur can readily react with Cu in a Cu/zeolite SCR catalyst forming stable CuSO_4 -like compounds ^[14-16]. This sulfur poisoning affects the redox properties of the Cu sites, severely inhibits NO oxidation and the subsequent formation of the adsorbed NOx complex, and ultimately decreases the SCR activity of the catalyst. Despite drastic reduction of sulfur content in diesel fuel in recent years, sulfur poisoning remains one of the most significant factors impacting the performance of Cu/zeolite catalysts. The poisoning effect of sulfur on the Cu/SAPO-34 catalyst has been reported by several groups ^[17,18]. Zhang et al ^[17] found the formation of $(\text{NH}_4)_2\text{SO}_4$ species that might poison the active sites and block the zeolite pores, which induce the inhibition of the SCR activity on Cu/SAPO-34 below 300 °C. Kumar et al ^[18] investigated the different impacts of SO_2 and SO_3 on Cu/SAPO-34 SCR catalysts. Obtained results indicated that the poisoning effect of different S species is almost identical or unobvious at low temperature (200 °C). While, at high temperature (400 °C), SO_3 has a substantial effect due to some temperature-activated chemical reaction taking place with catalyst material ^[14,18]. Overall, based on the literature, different sulfur poisoning mechanisms of NH_3 -SCR catalysts have been proposed. However the effect of sulphur poisoning on the structure and active sites of Cu/SAPO-34 has not been investigated. For direct automotive applications, it is very necessary to gain a better understanding of the sulphur poisoning properties for Cu/SAPO-34 catalyst. Understanding these properties would provide important information to improve the performance of sulphur resistance for meeting different fuel standards.

This study deals with an intensive investigation for the SO_2 poisoning on the

structure and active sites over Cu/SAPO-34 catalysts. The different sulphated samples were prepared by exposed to 112 ppm SO₂ for 5 h and 16 h/, or 336 ppm SO₂ for 16 h with 10% H₂O at 250 °C respectively. The total sulfur throughput corresponded to 100,000 kilometre and 3,200,000 kilometre sulfur-equivalent miles (assuming 15 ppm S fuel) or 3,200,000 kilometre sulfur-equivalent miles (assuming 50 ppm S fuel)^[15,16]. The nature and structure of the Cu/SAPO-34 catalysts were characterized by XRD, *ex-situ* DRIFTS, H₂-TPR and EPR. The kinetic analysis was used to study the influence of SO₂ poisoning of active sites. The mechanism of SO₂ poisoning over Cu/SAPO-34 catalysts was proposed.

2. Experimental

2.1. Catalyst preparation

The HSAPO-34 molecular sieve was synthesized by hydrothermal method from a gel with the molar composition Al₂O₃:SiO₂:P₂O₅:Morpholine:H₂O=1.0:0.6:1.0:2.0:60. Pseudoboehmite (68 wt% Al₂O₃), orthophosphoric acid (85 wt% H₃PO₄) and silica sol (25 wt% SiO₂) were used as the source of aluminium, phosphorus and silicon, respectively. Cu/SAPO-34 catalysts were synthesized by exchanging NH₄-SAPO-34 in copper sulfate solution. The detail synthesis procedures of the Cu/SAPO-34 catalysts had been reported in our former study ^[19]. The fresh supports or the Cu/SAPO-34 catalysts were hydrothermally treated at 750 °C for 4 h in 10% H₂O/air to get de-greened samples; the samples were named as SAPO-34 and Cu/SAPO-34, respectively.

In SO₂ poisoning process, Cu/SAPO-34 was heated from room temperature to 250 °C and exposed in 112 ppm SO₂ for 5 h or 16 h, or in 336 ppm SO₂ for 16 h with 10% H₂O/air at 250 °C respectively. The poisoned samples were named as Cu-112-5, Cu-112-16 and Cu-336-16 according to the concentration of SO₂ and treating time. Similarly, the support was heated from room temperature to 250 °C and exposed in 336 ppm SO₂, 10% H₂O/air for 16 h. The SO₂ poisoned support was named as SAPO-34-336-16h.

2.2. NH₃-SCR performance evaluation

The NH₃-SCR activity was performed at atmospheric pressure in a three-sleeve quartz reactor. The 100 mg catalysts (powder 60-80 mesh) mixed with 900 mg quartz sands were packed in the plug flow reactor and the temperature was controlled by a type K thermocouple inserted into the centre of the catalysts. The gas flow and volume hourly space velocities in NH₃-SCR activity experiments was controlled at 500 ml/min and 300,000h⁻¹, respectively. The inlet gases contained 500 ppm NO, 500 ppm NH₃, 5% O₂, 5% H₂O and 8% CO₂. The gas composition was controlled by mass flow controllers and the outlet concentrations were analysed by a Fourier Transform Infrared (FTIR) spectrometer (MKS-2030) equipped with a 5.11 m gas cell. The test temperatures were selected from 100 °C to 500 °C. The NO_x conversions were calculated by Eq. (1) which based on the inlet and outlet gas concentrations.

$$\text{NO}_x \text{ Conversion} = \frac{(\text{NO} + \text{NO}_2)_{\text{inlet}} - (\text{NO} + \text{NO}_2)_{\text{outlet}}}{(\text{NO} + \text{NO}_2)_{\text{inlet}}} \times 100\% \quad \dots\dots\dots (1)$$

The NH₃-SCR kinetic results of Cu/SAPO-34 catalysts were obtained in a differential reactor fitted with 25 mg catalyst and 125mg quartz sand. The samples particles were 80-100 mesh and the volume hourly space velocities (VHSV) was 3,600,000 h⁻¹ to eliminate internal and external diffusion, respectively. The samples were pre-treated in 5% O₂/N₂ at 300 °C before kinetic experiments. Since negligible effects of H₂O (g) and CO₂ in our previous study ^[12], the SCR kinetic experiments were performed without H₂O (g) and CO₂. The reaction gas consisted of 500 ppm NO, 500 ppm NH₃, 5% O₂ with N₂ as the balance. The kinetic steady-state measurements were obtained from 170 °C to 230 °C at 20 °C intervals and kept at each temperature for at least 1.5 h. By assuming plug flow reactor and free of diffusion limitations, the NH₃-SCR reaction rates can be calculated from the NO_x conversion by:

$$\text{rate} [\text{mol NO}_x \cdot \text{g}_{\text{cata}} \cdot \text{s}^{-1}] = \frac{X_{\text{NO}_x} [\%] \times F_{\text{NO}_x} [\text{L}(\text{NO}_x) \cdot \text{min}^{-1}]}{m_{\text{cata}} [\text{g}] \times 60 [\text{s} \cdot \text{min}^{-1}] \times 22.4 [\text{L} \cdot \text{mol}^{-1}]} [\text{mol NO}_x \cdot \text{g}_{\text{cata}} \cdot \text{s}^{-1}] \quad \dots\dots\dots (2)$$

X_{NO_x} = NO_x Conversion, [%];

F_{NO_x} = Flow Rate of NO_x, [L (NO_x)·min⁻¹]

2.3. Catalyst characterization

The Cu content was determined by ICP-AES (inductively coupled plasma and atomic emission spectrometry), and the Si, P, Al and S contents were determined by X-Ray Fluorescence (XRF). The Cu content of the Cu/SAPO-34 catalysts was 1.66 wt% and Al:Si:P ratio (1:0.22:0.83) was calculated by molar ratio of Al, Si and P by Al as the standard.

The XRD patterns were acquired using X'Pert Pro diffractometer operating at 40 kV and 40 mA with nickel-filtered Cu K α radiation ($\lambda=1.5418 \text{ \AA}$) in the range $5^\circ < 2\theta < 50^\circ$ with a step size of 0.02° . The BET surface area was determined from the linear portion of the BET plot by measuring the N₂ isotherm of the samples at 77 K using F-Sorb 3400 volumetric adsorption/desorption apparatus. Prior to the measurement, the samples were degassed at 150 °C under vacuum for 3 h (Table 1).

The Electron Paramagnetic Resonance (EPR) spectra were recorded on a Bruker ESP320 spectrometer. The Bruker ESP320E software and the special Bruker program were used for data analysis. Each spectrum was obtained by multiple scans to achieve a satisfied signal to noise ratio. Before these measurements, the samples were pre-treated in air at 300 °C for 1 h. Then X-band ($\nu= 9.78 \text{ GHz}$) EPR spectra were recorded at room temperature and the magnetic field was swept from 2000 Gauss to 5000 Gauss. The standard sample DPPH ($g=2.0036$) was used for calibration of the instrument error before every measurement. The location and the intensity of g factors were determined by Bruker's WINEPR program based on the $h\nu=g\beta H$, where h was Planck constant, H was the actual magnetic field, and β is Bohr magneton.

Temperature Programmed Reduction (TPR) experiments were performed in a U-shaped tubular quartz reactor. Prior to reduction, the samples (100 mg) were first treated at 300 °C under a flow of 30 ml/min 2% O₂/N₂ and kept for 30 minutes. Then, the samples were cooled down to room temperature following by purging in N₂ with a

flow of 30 ml/min. In the temperature programmed reduction process, the samples were measured in a flow of 5% H₂/N₂ (10 ml/min⁻¹) from 30 °C to 900 °C at a ramping rate of 10 °C·min⁻¹. The consumption of hydrogen was monitored by a thermal conductivity detector and combined by mass spectrometer (HIDEN HPR20). Diffuse reflectance infrared Fourier transform spectra (DRIFTS) was measured on a FTIR spectrometer (Nicolet 6700 FTIR) with a MCT detector at a resolution of 2 cm⁻¹, averaging 32 scans for each spectrum, using the OMNIC software. ZnSe windows were used in the commercial high-temperature vacuum diffuse reflectance chamber (Thermofisher). The *ex-situ* DRIFTS spectra were recorded in the range of 4000-400 cm⁻¹. Initially, the samples were treated at 300 °C in 1% O₂/He/Ar for 1 h executing to remove the adsorbed water and clean the surface before each measurement. The spectra of the catalysts were recorded at 150 °C in He/Ar atmosphere and the spectrum of KBr under the same condition was used as the background. For the SO₂-DRIFTS experiments, the fresh Cu/SAPO-34 was treated at 300 °C in 1% O₂/He/Ar for 1 h and then the sample was exposed to 0.1% SO₂ with 2% O₂ until stable, the experiment was conducted at 250 °C.

3. Results

3.1. XRD&BET

Fig. 1 shows the XRD patterns of fresh and SO₂ poisoned samples. All the samples present the typical chabazite structure and keep a high crystallinity, which meant that SO₂ poisoning did not destroy the structure of molecular sieves^[20,21]. Sulfur oxides are expected to have larger affinity to copper species compared with strong acid sites originating from the SAPO-34. However the formation of ammonium sulfate or ammonium bisulfate species does not change the CHA structure due to the amount of sulfate species is too small (< 2µm) and well dispersed on the supports. Furthermore, Cu/SAPO-34 catalysts with relatively small pores and one-dimensional pore structure have shown certain poisoning resistance to these deposits. The results of the BET

surface area (Table 1) show that both fresh and SO₂ poisoned samples keep a high surface area (around 540m²/g). It indicated that SO₂ poisoning does not obviously change the framework structure of Cu/SAPO-34 catalyst.

3.2. *Ex-situ* DRIFTS

In order to probe the effect of SO₂ poisoning on the SAPO-34 framework vibrations, the *ex-situ* DRIFT spectra was used to characterize the surface during exposure to SO₂ (As shown in Fig.2). The spectra in absorbance units are acquired after pretreating the samples at 300 °C to remove the adsorbed water and clean the surface. Peaks in the range of 2000 cm⁻¹-650 cm⁻¹ associated with the internal and external stretching vibrations of the SAPO-34 framework. The peaks in the 3800 cm⁻¹-3500 cm⁻¹ region are related to the OH group stretching vibration modes. The weaker bands at 3745cm⁻¹ and 3678 cm⁻¹ are assigned to P-OH and Si-OH species located on the external surface of the sample particles, respectively. Two stronger bands at 3627 cm⁻¹ and 3600 cm⁻¹ are assigned as the stretching mode of bridged OH groups Al-(OH)-Si, which are related to the Brønsted OH groups ^[7]. The result illustrates that there is no significant difference between the spectra of fresh and SO₂ poisoning SAPO-34 (Fig. 2a). So it is suggested that SAPO-34 support are insensitive to sulfur, since both of them shows acidic.

For the DRIFT spectra of Cu/SAPO-34 samples (Fig. 2b), two bands at 891cm⁻¹ and 844 cm⁻¹ appear, which are associated with an internal asymmetric framework vibration perturbed by copper cations ^[21, 22]. Noteworthy, the intensity of the two bands obviously decline with the different sulfide degree. It illustrates that sulfates/sulfites may combine with the copper cations, which influence the coordination environment and the content of active Cu²⁺ species.

3.3. Catalyst activity

NH₃-SCR performance of various catalysts is shown in Fig. 3. It can be seen that the fresh Cu/SAPO-34 sample shows the superior SCR activity during the whole

temperature range (100 °C-500 °C), while the NO conversion of all the SO₂ poisoned samples decline obviously. The relation between the average NO conversion loss with the S content of the SO₂ poisoned samples is showed in Fig.4. The largest decline of the NO conversion is about 32% for Cu-336-16h sample, while the S content is 35.625 μmol/g catalysts. For all the samples, the Cu loading and Si: Al: P ratio is consistent, the XRD and BET results also show that the framework structure of the support does not change after SO₂ poisoning. It suggested that the decline of the NH₃-SCR activity is attributed to the reduction of the active Cu species. According to the previous results [14,17,18], some SO₂ are released during the TPD for Cu/SAPO-34 catalyst exposure to SO₂. And ammonium-sulfate or ammonium-bisulfate species would be formed in the presence of NH₃. However the decomposition temperature of (NH₄)₂SO₄ is at around 300 °C, which is far less than the desorption temperature of SO₂ for the sulphated Cu/SAPO-34 catalyst. So the influence of ammonium-sulfate formed during the SCR reaction on the activity was inconspicuously.

3.4. H₂-TPR

To obtain more information on the copper species, H₂-TPR was carried out on the fresh catalysts and SO₂ poisoned Cu/SAPO-34 catalysts (As shown in Fig. 5). Two main peaks (denoted as A and B) of H₂ consumption for Cu/SAPO-34 sample and three main peaks (denoted as A, B and C) of H₂ consumption for SO₂ poisoned catalysts from 150 °C to 600 °C are observed. The peak at the lower temperature (peak A) represents the reduction of isolated Cu²⁺ to Cu⁺ [23-25], the moderate one (peak B) represents the reduction of CuO to Cu⁰ [23, 24]. The peak at around 450 °C represent the reduction of the deactivated Cu²⁺ species, which are close to those observed from the reduction of CuSO₄·5H₂O [26]. The peak above 650 °C (peak D) can be attributed to the reduction of sulfate species. H₂S is detected at around 650 °C for the SO₂ poisoned samples by MS (see Fig.6). Hence, there are three types of Cu species in all the SO₂ poisoned samples, including external surface CuO, isolated Cu²⁺ and deactivated Cu²⁺. It is worth noting that the valence of sulfur species is difficult to

specify from TPR results. It is worth noting that the valence of sulfur species is difficult to specify from TPR results. But the TPR experiment shows that the sulfur species occur on copper sites of the Cu/SAPO-34 materials, and this phenomenon is corroborated with the TG and *ex-situ* DRIFTS results.

3.5. EPR

EPR is an excellent technique for quantitatively identifying the amount of isolated Cu^{2+} ions and to probe the structure and coordination environment. Fig. 7 shows the EPR spectra of the fresh and SO_2 poisoned Cu/SAPO-34 catalysts performed at room temperature. Ham and Kim et al [27, 28] suggested that the isolated Cu^{2+} ions was octahedral coordinated to three framework oxygen atoms and three water molecules in Cu/SAPO-34. As shown in Fig. 7, the Cu^{2+} species load in all Cu/SAPO-34 samples display axial symmetry for all spectra. For all Cu/SAPO-34 samples, the characteristic signal peaks of isolated Cu^{2+} at $g_{\parallel}=2.373$ and $g_{\perp}=2.047$ are observed, which is characteristic of the Cu^{2+} species in site (I) (Cu^{2+} (I)) [29, 30], it illustrates that the location of the Cu^{2+} does not change after SO_2 poisoning. Four hyperfine splitting peaks (originated from the interaction of the Cu nuclear and unpaired electron) clearly observed from the spectra of the fresh Cu/SAPO-34. Simultaneously, the hyperfine splitting peaks of the SO_2 poisoned samples are not obvious. The strength of the peaks decline for the SO_2 poisoned samples, which mean the reduction of the content of the active isolated Cu^{2+} species.

4. Discussion

4.1 The effect of SO_2 poisoning on the structure of the Cu/SAPO-34

According to the sulfur content shown in Table 1 and the XRD patterns shown in Fig. 1, there is almost no sulfur exists on the SAPO-34 support after SO_2 exposure. In addition, the *ex-situ* DRIFT results illustrate that SO_2 poisoning has a less pronounced influence on the structure of the SAPO-34 support. It can be concluded that SO_2 could not influence the crystal and texture structure of the support because SO_2 is difficult to

interact with HSAPO-34. In good agreement with results of Kumar et al^[18], very little SO₂ was absorbed on the SAPO-34 support due to both of them showing acidity. However, for the Cu/SAPO-34 catalysts, the coordination environment of Cu species has a significant change according to the decline of the strength of the two bands at 891cm⁻¹ and 844 cm⁻¹ by the *ex-situ* DRIFT results (Fig. 2). It suggested that the varying states of copper species among the different sulfate samples resulted in noticeable SCR activity degradation.

4.2 The effect of SO₂ poisoning on the Cu species

According to the results of H₂-TPR, there are three types of copper species in all the SO₂ poisoned Cu/SAPO-34 samples. However, the intensity of each H₂ consumption peak is significantly different according to the degree of SO₂ treatment. It indicates that the SO₂ poisoning influence the distribution of Cu species. According to the TPR quantification results (As shown in Fig.8), all the samples show the similar total amount of copper. Noteworthy, the content of the CuO species is basically unchanged after SO₂ exposure. However the amount of the Cu²⁺ decline with the aggravation of the SO₂ poisoning. In good agreement with EPR results, Cu²⁺ is more active than CuO species, being thus it is easier for electrons transferring. Fig. 9 shows the concentration of isolated Cu²⁺ ions semi-quantified by double integrating the EPR spectroscopy. It is observed that the amount of Cu²⁺ decline apparently after SO₂ exposure. According to the TPR results, the reduced Cu²⁺ is due to the partly deteriorated by the S species and eventually changed into the sulfate/sulfite species. Lavalley^[26] also found that the sulfates formed on copper sides by TPR. As the amount of S species is low in the SO₂ poisoned samples, the kind of sulfur species is difficult to specify from *ex-situ* DRIFTS results.

The thermal gravimetric experiments were conducted for all samples (As shown in Fig.S1). The amount of sulfate species for samples of different sulfate degree were calculated and shown in Fig 10. It is obviously that the amount of sulfate species increased with the time and the concentration of SO₂ exposure.

4.3 The effect of the SO₂ poisoning on the NH₃-SCR activity

The kinetic NH_3 -SCR reaction was performed between 170 °C to 230 °C, at which temperatures the NO conversion is less than 20%. Fig. 11 presents the Arrhenius plots of the SCR reaction rates over SO_2 poisoned Cu/SAPO-34 samples. At each fixed temperature, the reaction rate decreases with increased sulfide degree. It indicates that SO_2 exposure makes part of active Cu^{2+} deactivation. The relationship between the molar ratio of S/ Cu^{2+} and the rate of NO conversion over all Cu/SAPO-34 catalysts is shown in Fig.12. The result shows that the lowest occupation of S species per Cu^{2+} ion on the catalysts is about 13%. However the reaction rate for NO conversion immediately decreases from 16.85×10^{-5} to 8.61×10^{-5} mmol/g/s. Further, the S/ Cu^{2+} ratio and the reaction rate maintain a linear regular on the SO_2 poisoned samples. It reveals that the catalyst is very sensitive to SO_2 exposure.

According to the kinetic results, all the samples present a similar apparent activation energy ($E_a=33.99\text{kJ}\cdot\text{mol}^{-1}$), which is coincident with our previous result ($33.6\text{kJ}\cdot\text{mol}^{-1}$) for the ion-exchange Cu/SAPO-34 catalysts [12]. It illustrates that SO_2 poisoning does not change the SCR reaction mechanism. Noteworthy, the samples show different pre-exponential factor (A), illustrating the decline of active sites content. According to our previous study, the isolated Cu^{2+} is the activity site of Cu/SAPO-34 for NH_3 -SCR reaction [12]. So it can be concluded that SO_2 may attack the isolated Cu^{2+} to form cupric sulfates/sulfites species, which result in the active Cu^{2+} species lose its ability involving in the reaction.

Fig. 13 presents the results of SO_2 -DRIFTS of Cu/SAPO-34, the two bands of Cu^{2+} species at 890cm^{-1} and 845cm^{-1} occur at about 3 min. It illustrates that SO_2 adsorb on the Cu^{2+} species immediately (3 min) as soon as SO_2 is exposure to the Cu/SAPO-34 sample. Combining the above data, it was concluded that the mechanism of SO_2 poisoning could be concluded as shown in Scheme 1. SO_2 is acidic and the isolated Cu^{2+} is electronegative, the gaseous SO_2 molecule is easy to adsorb on Cu^{2+} . Then SO_2 may translate into sulfite on the Cu^{2+} side. The Cu^{2+} and sulfur species also contain the characteristic of the coordinate covalent bond, where Cu^{2+} and sulfur species may act as a Lewis acid and base, respectively [31]. Moreover, in the presence of gaseous oxygen, Cu^{2+} firstly performs catalytic oxidation of SO_2 to SO_3 , which

then forms sulfate on the copper site^[32]. Kim et al^[33] found that the translation of SO₂ to SO₃ is much higher reaction rate for copper containing catalyst than for copper free ones. So both sulfates and sulfites exist on the SO₂ poisoned samples. As we known, SAPO-34 is a structural equivalent of chabazite zeolite, which has channel dimensions 4.3 Å×4.3 Å and formed by 8-membered oxygen ring^[34]. Since the bond distance between S and O atoms in SO₄²⁻ is known to be 1.49 Å^[35], the diagonal length of O-S-O bond in the SO₄²⁻ anion is approximately 2.58 Å^[33]. SO₂ is able to diffuse into the channels of SAPO-34 to interact with Cu²⁺ (0.73 Å) and form SO₄²⁻. Since Cu²⁺ species in the cage of the zeolite and exist in an isolated environment, they could interact with the sulfates/sulfites species to form cupric sulfates/sulfites at the original position of the catalyst.

5. Conclusions

The SAPO-34 support and the Cu/SAPO-34 catalysts prepared by ion-exchange method are treated with different SO₂ concentrations (112 ppm and 336 ppm) and time (5 h and 16 h) at 250 °C. The framework of SAPO-34 does not change after SO₂ poisoning. The NH₃-SCR performance deactivation observed in the current study is attributed to the loss of active Cu sites in the catalyst due to the presence of sulfur. And the coordination of Cu²⁺ species in Cu/SAPO-34 samples is affected by SO₂ from *ex-situ* DRIFTS. The TPR and EPR results further confirm the amounts of Cu²⁺ in SO₂ poisoned samples decline, and they may transform into cupric sulfates/sulfites. Moreover, the kinetic results demonstrate the SO₂ poisoning cannot influence the reaction mechanism of NH₃-SCR reaction over Cu/SAPO-34 catalysts.

Acknowledgements

The authors are grateful to the financial support from the GM Global Research & Development (RD-07-312–NV487).

Supporting Information Available: Some related figures are shown in the supporting information.

References

- [1] D. W. Fickel, E. D'Addio, J. A. Lauterbach and R. F. Lobo, *Appl. Catal., B*, 2011, 102, 441.
- [2] R. Kefirov, A. Penkova, K. Hadjiivanov, S. Dzwigaj and M. Che, *Microporous Mesoporous Mater.*, 2008, 116, 180.
- [3] S. Brandenberger, O. Kro"cher, A. Tissler and R. Althoff, *Catal. Rev. Sci. Eng.*, 2008, 50, 492.
- [4] I. Bull, R. S. Samuel, W. M. Jaglowski, G. S. Koermer, A. Moini, J. A. Patchett, W. Xue and P. Burk, *US Pat. 106519 A1*, 2008.
- [5] Ja Hun Kwak, Russell G. Tonkyn, *J. Catal.* 2010, 275, 187.
- [6] Dustin W. Fickel, Elizabeth D'Addio, Jochen A. Lauterbach, Raul F. Lobo, *Appl. Catal. B*. 2011, 102, 441.
- [7] P. G. Blakeman, E. M. Burkholder, H.Y. Chen, J. E. Collier, J. M. Fedeyko, H. Jobson, R. R. Rajaram, *Catal. Today*, 2014, 231, 56.
- [8] I. Bull, W.M. Xue, P. Burk, R. S. Boorse, W. M. Jaglowski, G. S. Koermer, A. Moini, J. A. Patchett, J. C. Dettling, M. T. Caudle, Copper CHA zeolite catalysts. *US Patent 7,610,662*, 2009.
- [9] P. J. Andersen, J. E. Bailie, J. L. Casci, H.-Y. Chen, J. M. Fedeyko, R. K. S. Foo, R. R. Rajaram, Transition metal/zeolite SCR catalysts. *US Patent 2010/0290963*, 2010.
- [10] S. T. Korhonen, D. W. Fickel, R. F. Lobo, B. M. Weckhuysen, A. M. Beale, *Chem. Commun.* 2011, 47, 800.
- [11] F. Gao, E. D. Walter, N. M. Washton, J. Szanyi, C. H. F. Peden, *ACS Catal.* 2013, 3, 2083.
- [12] J. Xue, X. Wang, G. Qi, J. Wang, M. Shen, W. Li, *J. Catal.* 2013, 297, 56.
- [13] K. Arakawa, S. Matsuda, H. Kinoshita. *Appl. Surf. Sci.* 1997, 121/122, 382.
- [14] Y. Cheng, C. Lambert, D. H. Kim, et al. *Catal. Today*, 2010, 151, 266.
- [15] Y. S. Cheng, C. Montreuil, G. Cavataio, C. Lambert, *SAE 2008-01-1023*, 2008

- [16] Y. S. Cheng, C. Montreuil, G. Cavataio, C. Lambert, SAE 2009-01-0898, 2009
- [17] L. Zhang, D. Wang, Y. Liu, K. Kamasamudram, J.H. Li, W. Epling, Appl. Catal. B.2014, 156-157, 371.
- [18] A. Kumar, M. A. Smith, K. Kamasamudram, N. W. Currier, H.M. An, A. Yezerets. Catal. Today. 2014,231,75
- [19] S.K.Fan, J.J.Xue, T. Yu, et al, Catal. Sci. Technol., 2013,3, 2357
- [20] A. Buchholz, W. Wang, M. Xu, A. Arnold, M. Hunger, Micropor. Mesopor. Mater. 2002,56,267.
- [21] P.E. Fanning, M.A. Vannice, J. Catal. 2002,207,166.
- [22] G.D. Lei, B.J. Adelman, J. Sárkány, W.M.H. Sachtler, Appl. Catal. B. 1995,5,245.
- [23] C. Torre-Abreu, M.F. Ribeiro, C. Henriques, G. Delahay, Appl. Catal. B. 1997,14,261.
- [24] M. Richter, M.J.G. Fait, R. Eckelt, Appl. Catal. B. 2007,73, 269.
- [25] A. Sultana, T. Nanba, M. Haneda, M. Sasaki, H. Hamada, Appl. Catal. B. 2010,101,61.
- [26] M. Ziółek, I. Sobczak, I. Nowak, M. Daturi, J.C. Lavalley, Top Catal. 2000, 11/12,343.
- [27] S.W. Ham, H. Choi, I.S. Nam and Y.G. Kim, Catal. Today. 1992,11, 611.
- [28] M.H. Kim, I.S. Nam and Y.G. Kim, Appl. Catal. B. 1995,6, 297.
- [29] M. Zamadics, X. Chen, L. Kevan, J. Phys. Chem. 1992,96,2652.
- [30] M. Zamadics, X. Chen, L. Kevan, J. Phys. Chem. 1992,96,5488.
- [31] J. N. Armor, Y. Li. Appl. Catal. B, 1995, 5, 257.
- [32] M. Waqif, Saur, J. C. Lavalley, J. Phys. Chem. 1991,95,4051
- [33] M. H. Kim, I. S. Nam, Y. G. Kim. J. Catal., 1998, 179, 350.
- [34] B. M. Lok, C. A. Messina, R. L. Patton, R. T. Gajek, T. R. Cannon and E. M. Flanigen, Crystalline silicoaluminophosphates. US Patent 4440871, 1984.

[35] A. Bianconi, X-ray Absorption: Principles, Applications, Techniques of EXAFS, SEXAFS, and XANES, Wiley, 1988, p. 573.

Figure/ Table Captions

Table 1 Sulfur content and BET area of all the samples

Fig. 1 XRD patterns of all the fresh samples and SO₂ poisoned samples

Fig. 2 *Ex-situ* DRIFTS spectra of all the fresh samples and SO₂ poisoned samples

Fig. 3 NO conversions as a function of reaction temperature; reaction condition: 500ppmNO, 500ppmNH₃, 5% O₂, 8% CO₂, 3% H₂O balanced with N₂; the flow rate: 500 mL/min; GHSV: 300,000 h⁻¹, catalyst weight: 100mg

Fig. 4 The relationship between S content and average loss of NO conversion over SO₂ poisoned Cu/SAPO-34

Fig. 5 H₂-TPR profiles for the fresh sample and SO₂ poisoned samples. Conditions: 5% H₂ balanced with N₂. Flow rate: 10 ml·min⁻¹. Ramping rate: 10 °C·min⁻¹. “Dash line” represents for the fitting results.

Fig. 6 The partial pressure of H₂S for fresh and SO₂ poisoned samples

Fig.7 EPR spectra of fresh sample and SO₂ poisoned samples at room temperature after pretreating 60 minutes at 300 °C.

Fig. 8 Amount of Cu species quantified by the H₂-TPR profile.

Fig.9 Concentration of isolated Cu²⁺ ions semi-quantified by double integrating the EPR spectroscopy

Fig. 10 The amount of sulfate species quantified by TG

Fig. 11 Arrhenius plots of the SCR reaction rates at 170 °C-230 °C over fresh and SO₂ poisoned samples. The in-let gas composition: 500 ppm NO, 500 ppm NH₃, 5% O₂/N₂. Flow rate: 1.5 L·min⁻¹. GHSV: 3600,000 h⁻¹. Catalysts weight: 25 mg

Fig. 12 The relationship between the molar ratio of S/Cu²⁺ and the rate of NO

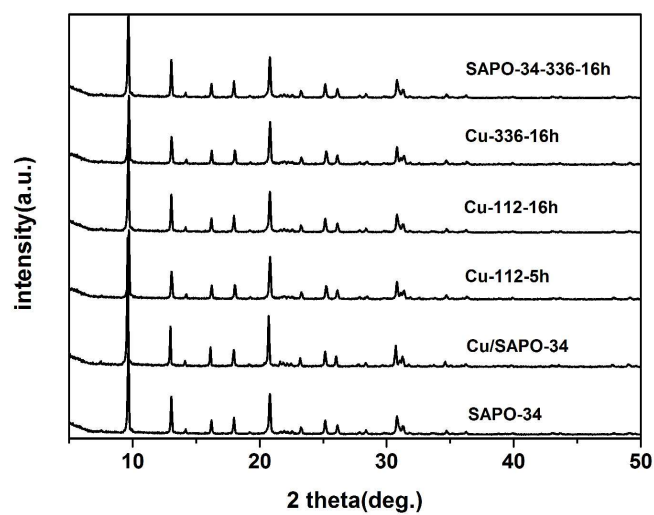
conversion over the SO₂ poisoned samples

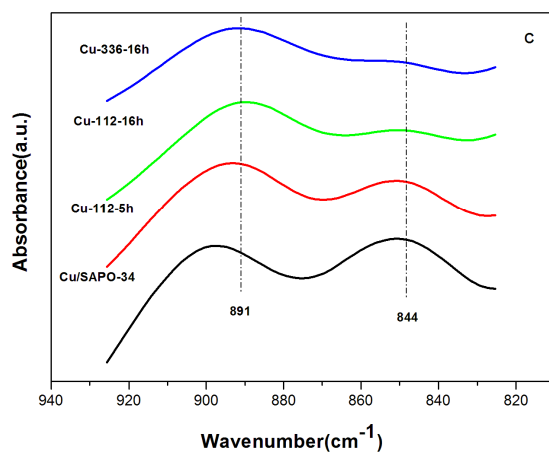
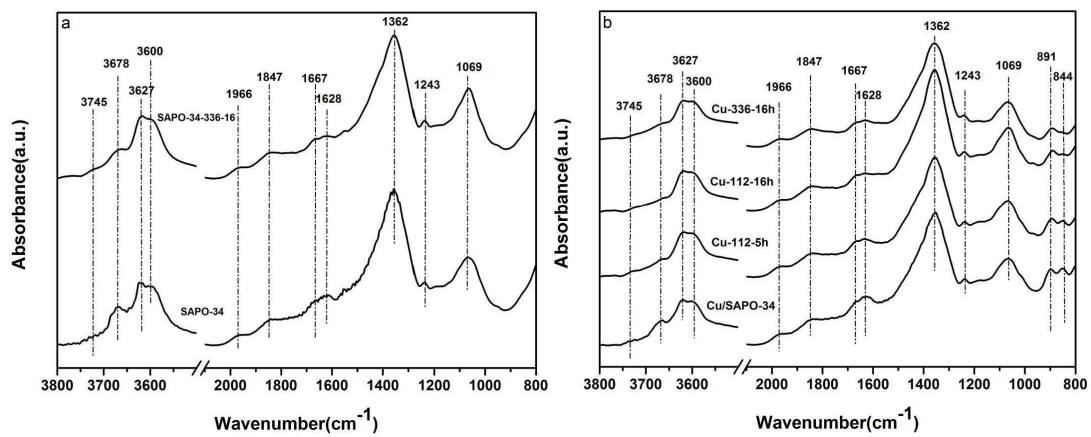
Fig. 13 DRIFT spectra of Cu²⁺ species on Cu/SAPO-34 catalysts during exposure to SO₂ + O₂

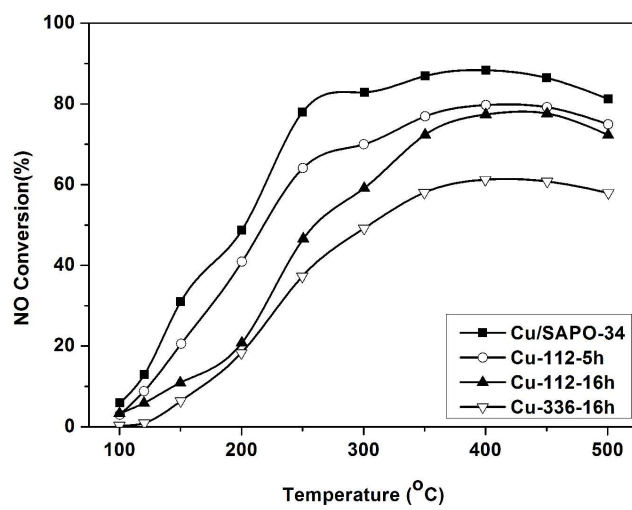
Scheme 1 The mechanism of SO₂ poisoning on NH₃-SCR reaction over Cu/SAPO-34 catalysts

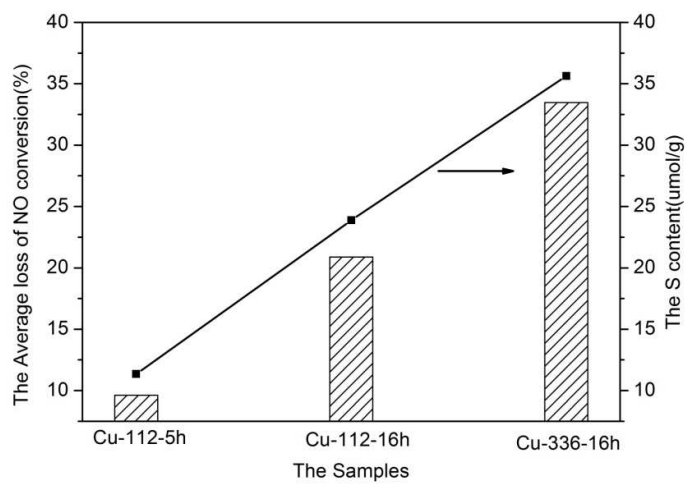
Table1 Sulfur content and BET area of all the samples

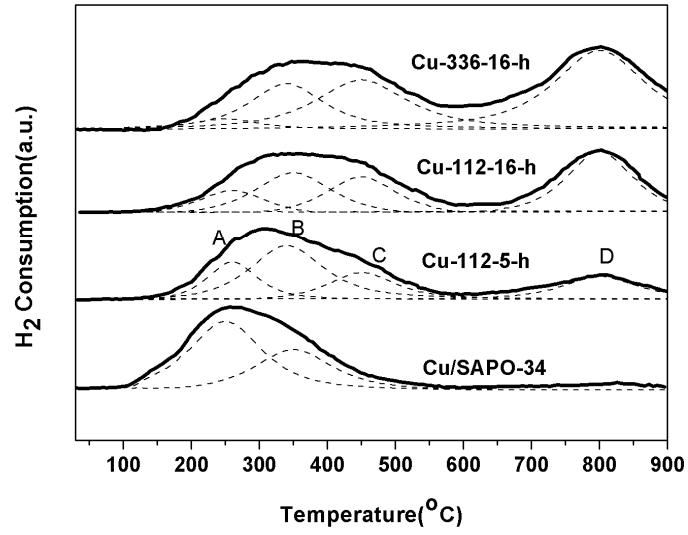
Sample	Sulfur content ($\mu\text{mol/g Cu/SAPO-34}$)	BET area (m^2/g)
SAPO-34	0	539.5
SAPO-34-336-16	0	537.1
Cu/SAPO-34	0	570.7
Cu-112-5	11.3	557.7
Cu-112-16	23.9	546.1
Cu-336-16	35.6	538.2

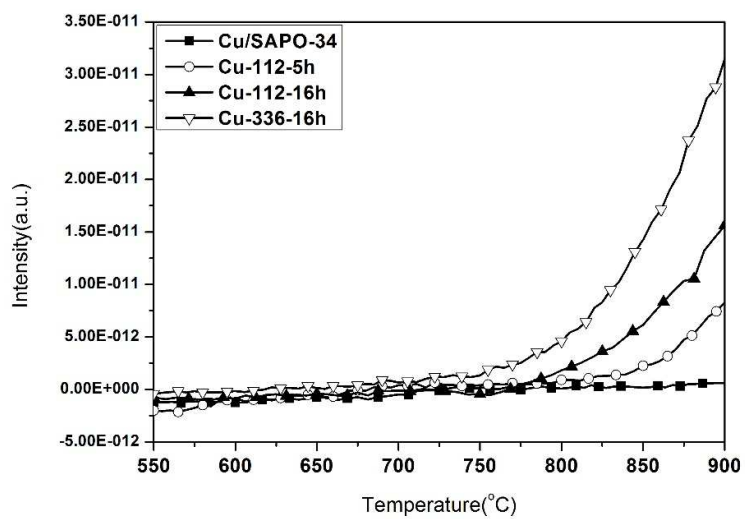


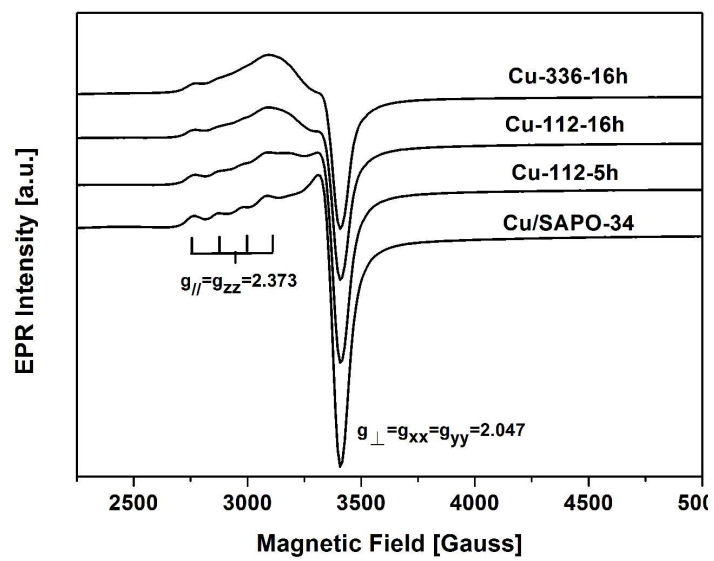


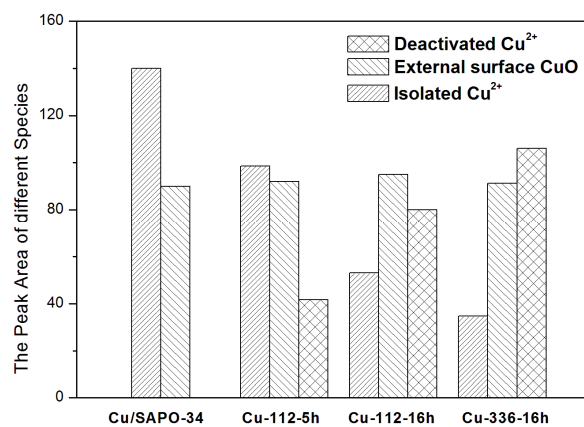


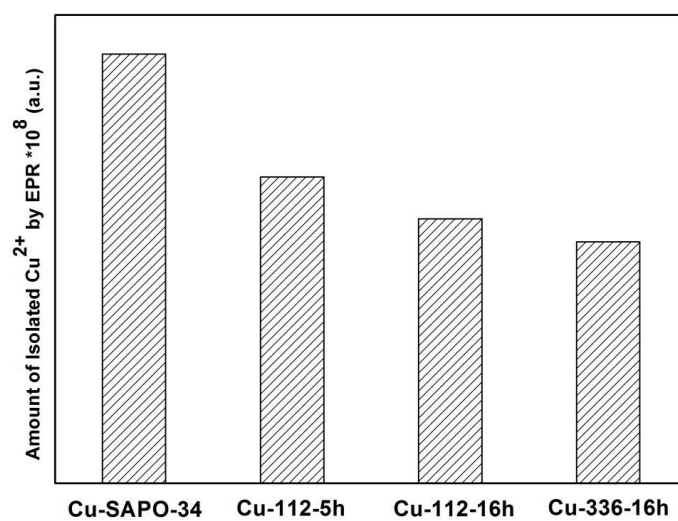


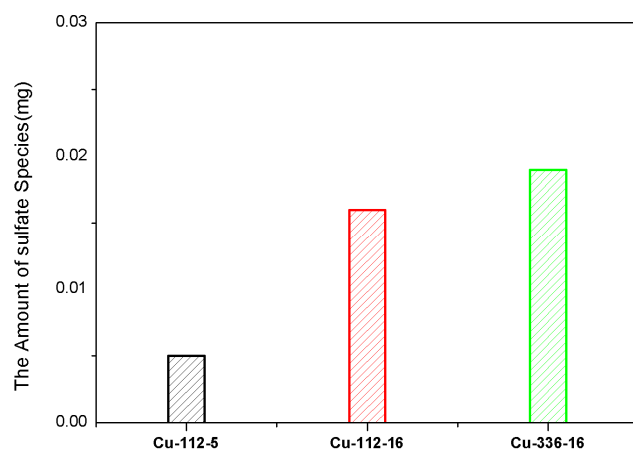


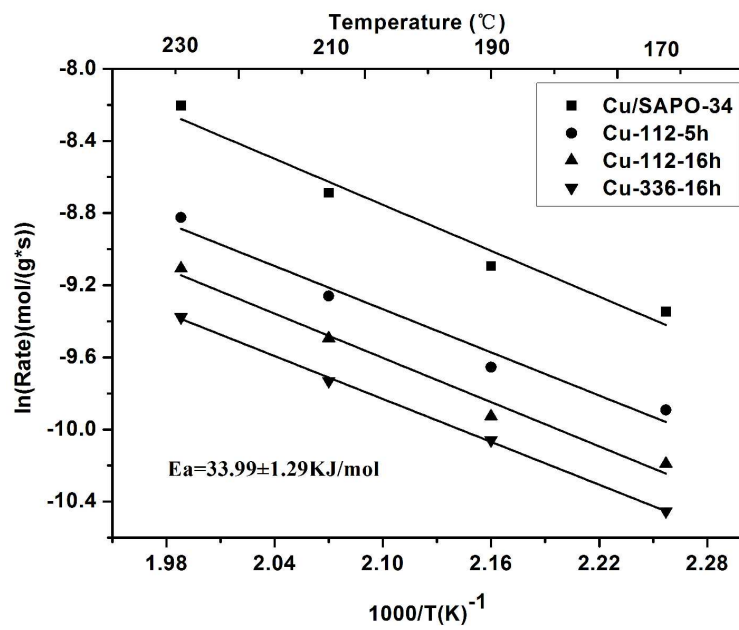


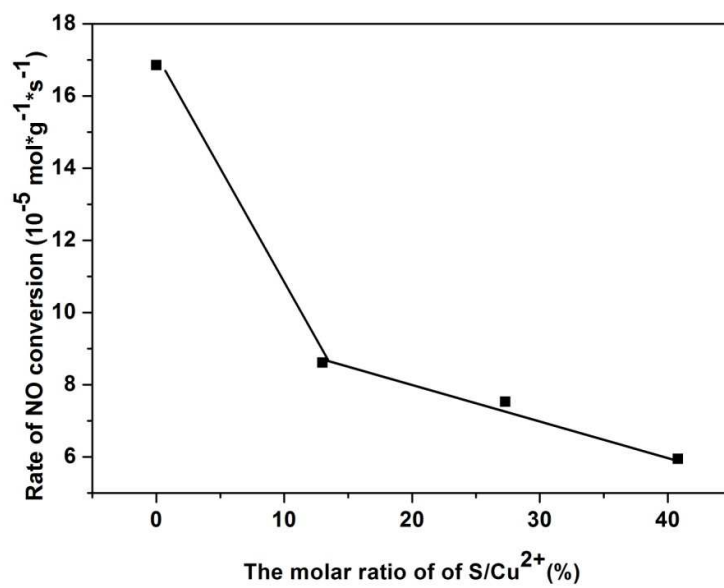


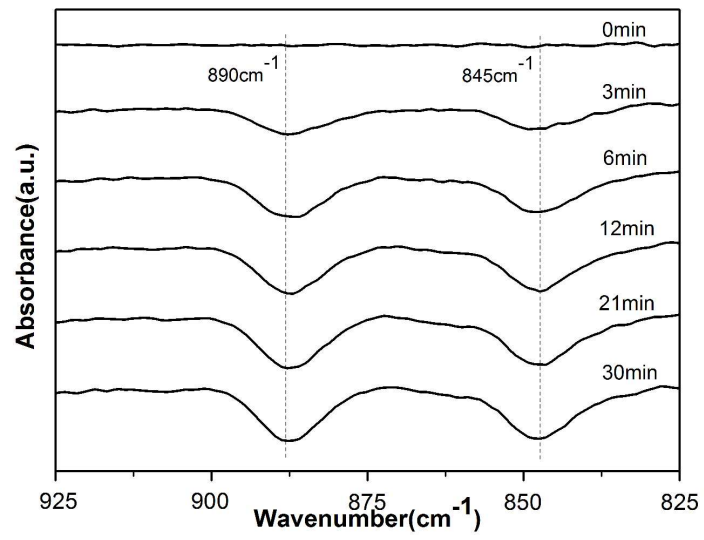


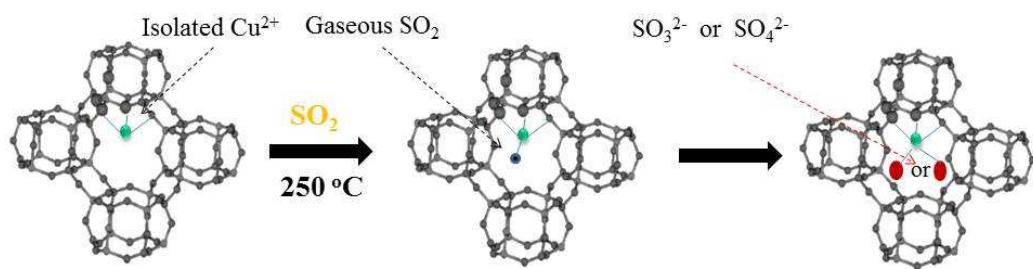












Supporting information

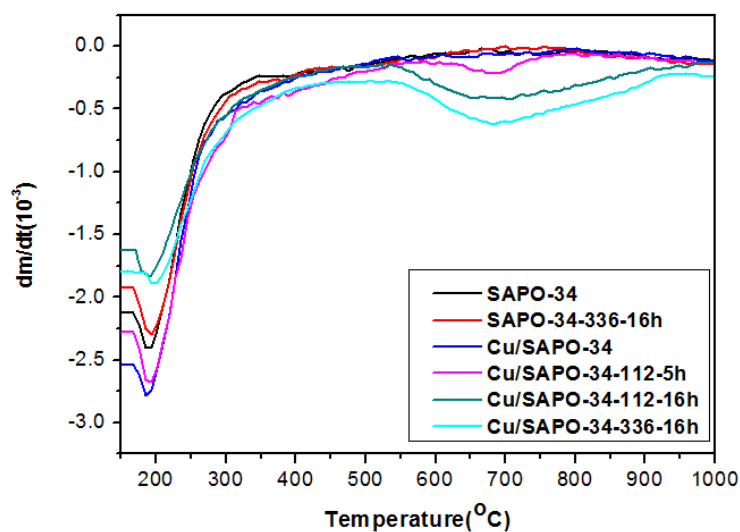


Fig.1 Derivative TGA data of weight loss of all SAPO-34 samples during temperature programmed process in 20 % O₂/N₂ atmosphere

Thermal gravimetric experiments were conducted on METTLER TOLEDO thermal gravimetric analysis. 10 mg samples were heated in a mixture gas flow contained N₂ (25 ml/min) and O₂ (5 ml/min) at a heating rate of 10 °C/min from ambient temperature to 1000 °C.